Chapter 15

User-Friendly Quantum Mechanics: Applications for Drug Discovery

Martin Kotev, Laurie Sarrat, and Constantino Diaz Gonzalez

Abstract

Quantum mechanics (QM) methods provide a fine description of receptor-ligand interactions and of chemical reactions. Their use in drug design and drug discovery is increasing, especially for complex systems including metal ions in the binding sites, for the design of highly selective inhibitors, for the optimization of bi-specific compounds, to understand enzymatic reactions, and for the study of covalent ligands and prodrugs. They are also used for generating molecular descriptors for predictive QSAR/QSPR models and for the parameterization of force fields. Thanks to the continuous increase of computational power offered by GPUs and to the development of sophisticated algorithms, QM methods are becoming part of the standard tools used in computer-aided drug design (CADD). We present the most used QM methods and software packages, and we discuss recent representative applications in drug design and drug discovery.

Key words Quantum mechanics, Quantum chemistry, DFT, SEQM, Drug discovery, Drug design, CADD, Binding affinity, Protein-ligand interaction, Reaction mechanism, Hit identification, Hit to lead, Lead optimization, QM/MM, Molecular dynamics, Virtual screening, QSAR, FMO

1 Introduction

It has almost been a century after publishing the famous quantum mechanical (QM) equation $H\psi\left(\vec{r}\right) = E\psi\left(\vec{r}\right)$ of E. Schrödinger and more than 20 years since the Nobel Prize in Chemistry was awarded "to Walter Kohn for his development of the density-functional theory and to John Pople for his development of computational methods in quantum chemistry." Today QM calculations are used routinely in almost every aspect concerning the computer-aided drug design (CADD) techniques. Initially, QM calculations were mainly and broadly applied to chemistry problems, due to smaller system size. With gradual increase of supercomputers' performance and graphics processing unit (GPU) implementations, QM calculations were performed for a variety of complex chemical, biochemical, and biomolecular systems. Applications in CADD

Alexander Heifetz (ed.), *Quantum Mechanics in Drug Discovery*, Methods in Molecular Biology, vol. 2114,
https://doi.org/10.1007/978-1-0716-0282-9_15,

include calculations at the following level of theory: semi-empirical quantum mechanical (SEQM) methods, Hartree-Fock (HF) approach, post-Hartree-Fock (pHF) methods, and density functional theory (DFT) methods. Hybrid quantum mechanics/molecular mechanics (QM/MM) methods are also widely used in CADD techniques.

2 Methods and Software Packages

2.1 Methods

Solving the Schrödinger equation, even for very simple systems, has led to the development of numerous approximations implemented in different QM methods which can describe all systems of interest today, such as organic, bioorganic, inorganic molecules and metal ions. Depending on the theory used, and the level of the simplification (the number and type of approximations), as aforementioned, we may summarize all QM methods into four major groups: SEQM, HF, pHF, and DFT. Although a specific combination, QM/MM approaches always include at least one of the four groups of QM methods. After finding the approximate solutions of the Schrödinger equation, we can obtain different measurable properties for the studied system [1–3].

The fastest and the most approximated approaches are SEQM methods. Around three orders of magnitude faster than HF calculations, they ignore some terms and replace others by empirical parameters to fit experimental heats of formation, dipole moments, and geometries. The most used SEQM are NDDO, MNDO, AM1, SAM1, RM1, PM3, PDDG/PM3, PDDG/MNDO, PM6, PM7, and OM2. Some of them were developed by John Pople, then many by Michael Dewar and lately by James J. P. Stewart group. SEQM undergo frequent improvement and revival and therefore stay quite popular on the scene [4–13].

Next in the order of increasing complexity (slow performance/high accuracy) is the HF method. The main approximation (among several others) assumes that each electron interacts with an average field of all other electrons in the system, thus reducing a many-body to a one-body problem. QM methods solve the Schrödinger equation representing the electron wave function by a set of finite number functions called basis functions (basis set). The quality of the solution is improved by a higher number of basis set functions. Usually for small drug molecules, we can get reasonable geometries with two basis functions for each valence electron and one for the core electrons. The most used are Pople basis sets, i.e., 3-21G, 6-31G, or 6-311G, where we may add also for some cases polarization functions (generally marked with *) and/or diffuse functions (denoted with +) study [1–3, 14, 15]. Polarization and diffuse-type functions could be added on heavy atoms and/or on hydrogens. Other widely used basis sets are developed by Dunning and

co-workers (correlation-consistent basis sets) [16–18]. Dunning series are noted as cc-pVNZ, where N could be D, T, Q, 5, 6,... (D is double, T is triple, and so on) and "cc-p" stands for "correlation-consistent polarized" and the V for valence basis sets. Diffuse function can also be added to Dunning basis set and denoted with "aug-" prefix. We should define basis sets also for all pHF and DFT methods. The minimal basis set for each SEQM is defined by the method itself; that is why basis sets for SEQM are not explicitly specified.

Post-HF methods [1–3] were developed to overcome the main approximation in the HF by adding electron correlation. These QM methods are more accurate compared to HF methods but they are more computationally expensive by orders of magnitude, compared to HF and DFT. The simplest way to correct HF is the second order of Møller-Plesset perturbation theory method or MP2 [19], and it is the most used pHF method due to its acceptable cost. However, the accuracy of MP2 method is considered worse compared to DFT methods, despite the slower performance. Coupled-cluster pHF method presents some of the most accurate calculations for small molecules [20]. The pHF method CCSD (T) known as the gold standard in quantum chemistry [21] is an abbreviation for "coupled-cluster calculations with single, double, and perturbative treated triple excitations."

DFT method study (as it is abbreviated in the name of the theory) [1–3, 22, 23] defines the properties of a many-electron system as functions of another function (functionals); this function is the electron density, and it is dependent from the three Cartesian coordinates. In the HF methods, the wave function (Ψ in the Schrödinger equation) also depends on three coordinates, but for each electron in the system. A number of DFT functionals have been developed, e.g., BP86, PBE, M06-L, M06-2X, B3LYP [24–28], and many others. One of the most used functionals for organic molecules is the hybrid B3LYP: Becke three-parameters is the exchange functional, and Lee, Yang, and Parr is the correlation functional. The three Becke parameters are derived from a fitting to a set of atomization energies, ionization potentials, proton affinities, and total atomic energies [26].

The main question for a scientist in order to decide which QM method to use for a CADD problem is the computational cost/effectiveness ratio that has to apply to a particular system of interest. Small drug molecule partial atomic charges, geometries and/or energies of different conformations, preferred tautomeric states in solution, covalent bonds, and electron transfer issues need to be evaluated according to the desired accuracy, and each could be solved by different QM method.

Table 1
Twenty of the most used software for QM calculations

Software package	SEQM	HF	pHF	DFT	License type	GPU	Internet link
ADF	Yes	Yes	No	Yes	Comm	Yes	www.scm.com
AMPAC	Yes	No	No	No	Acad	No	www.semichem.com
CASTEP	No	Yes	No	Yes	Acad/Comm	No	www.castep.org
CP2K	Yes	Yes	Yes	Yes	FOSS	Yes	www.cp2k.org
DIRAC	No	Yes	Yes	Yes	Acad	No	www.diracprogram.org
GAMESS (UK)	Yes	Yes	Yes	Yes	Acad/Comm	Yes	www.cfs.dl.ac.uk
GAMESS (US)	Yes	Yes	Yes	Yes	Acad	Yes	www.msg.chem.iastate.edu/gamess
Gaussian	Yes	Yes	Yes	Yes	Comm	Yes	www.gaussian.com
HyperChem	Yes	Yes	Yes	Yes	Comm	No	www.hyper.com
Jaguar	No	Yes	Yes	Yes	Comm	No	www.schrodinger.com/jaguar
MOLCAS	Yes	Yes	Yes	Yes	Acad/Comm	Yes	www.molcas.org
MOLPRO	No	Yes	Yes	Yes	Comm	Yes	www.molpro.net
MOPAC	Yes	No	No	No	Acad/Comm	Yes	www.openmopac.net
MPQC	No	Yes	Yes	Yes	FOSS	No	www.mpqc.org
NWChem	No	Yes	Yes	Yes	FOSS	Yes	www.nwchem-sw.org
Q-Chem	Yes	Yes	Yes	Yes	Comm	Yes	www.q-chem.com
QSite	No	Yes	Yes	Yes	Comm	No	www.schrodinger.com/QSite
Spartan	Yes	Yes	Yes	Yes	Comm	No	www.wavefun.com
TURBOMOLE	No	Yes	Yes	Yes	Comm	No	www.turbomole.com
VASP	No	Yes	Yes	Yes	Acad/Comm	Yes	www.vasp.at

License types include academic, commercial, and FOSS (free and open-source software)

2.2 Software Packages

In the past three or more decades, numerous QM software was developed with different level of theory and basis set implementation. In general, we can sort them by included methods. Most of the QM software now includes different combinations of SEQM, HF, pHF, and DFT methods. The use of a specific software is also related to its license: academic, commercial, and free and open source. Academic software license is possible to be acquired upon request, free of charge for academic institutions. Table 1 shows general overview of 20 of the most used software packages for QM calculations. In the past 10 years, company such as NVIDIA introduced video cards for scientific calculations. Molecular modeling calculations on GPU, including QM, have been gaining interest in the recent years due to the accelerated performance compared to

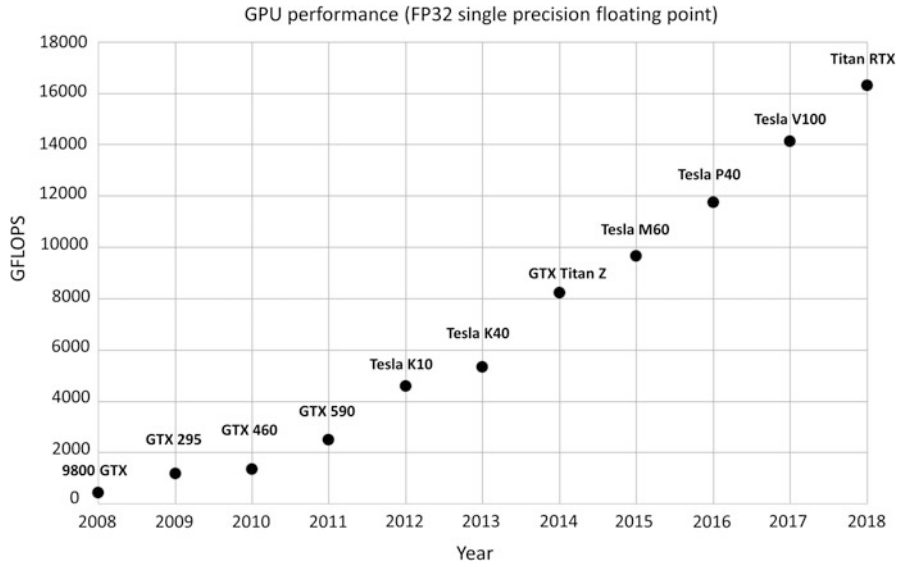

Fig. 1 Performance of GPUs, from year 2008 to 2018, in GFLOPS (10^9 floating point operations per second), for FP32 single-precision floating point calculations. The GPU models are shown above the corresponding dots. A 38-fold increase in computational power has been observed over 10 years. Data taken from https:/www.techpowerup.com/gpu-specs/

the standard CPU based. Figure 1 displays the performance of some of the best GPUs per year for the last decade, showing approximately 40-fold increase.

3 Application Domains

Computer-aided drug design (CADD) is commonly integrated in drug discovery and drug design processes [29–31]. The use of QM methods in CADD has increased during the last decade, especially due to breakthrough in computer hardware and the development of new algorithms [32–34]. QM methods provide accurate estimation of energies, electronic polarization effects, charge transfer, metal coordination, and bond formation and cleavage [35]. They allow reliable modeling and simulation of complex ligand-receptor systems, thus opening new possibilities for the study of difficult therapeutic targets and for the efficient development of optimized and selective drugs. We present and discuss diverse applications of QM in drug discovery and drug design, considering one or few examples by domain. For each application type, other examples are reported in Table 2.

3.1 QM/MM MD

Some of the most powerful approaches in the computational chemistry and in the drug design for studying protein-ligand and DNA-ligand interactions are the hybrid QM/MM methods and in particular QM/MM MD simulations [36, 37]. Together with

Table 2
Examples of various applications of QM-based methods in drug design and drug discovery

Applications	Papers
QM/MM MD	[90–92]
Parametrization of force fields	[93–96]
Protein structure refinement	[97–100]
Virtual screening	[101–103]
Protein-ligand affinity prediction	[104–109]
Identification of key drivers of protein-ligand binding	[110–113]
Protomer/tautomer states	[114–118]
Cation-π and π-π interactions	[119–122]
Bioactive conformations	[123–126]
Bi-specific inhibitors	[127–129]
Covalent compounds	[130–134]
Prodrugs	[135–139]
Reaction mechanisms	[140–146]
Drug metabolism	[147–150]
QSAR models	[151–153]
Molecular quantum similarity	[154, 155]
Enzyme design	[156–159]

the standard MD simulations, they represent two computationally expensive approaches in CADD, which recently could significantly benefit from the implementation of the GPU software and hardware.

Besides the routine use of QM methods such as calculating more accurate partial atomic ligand charges (like RESP method, [38]) for classical MD simulations in SBDD [39–41], in the past two decades, we have seen more computational chemists using QM/MM simulations [42–44]. In general, scientists treat a limited but important space of the protein (or DNA)-ligand complexes with higher accuracy at QM (but also SEQM) level. This important area could include the ligand (small peptide or small molecule) in case of a complex and the surrounding close environment—closest residues in a receptor pocket. The area can be an enzyme's active site where enzymatic cleavage reactions happen or a site with a covalent bonding possibility [45] or simply a pocket where non-covalent small drug molecules bind. The rest of the system, which is a huge part, is treated at a less accurate level using a classical force field (FF), the same as the ones in standard MD simulations

[36, 37, 42–44]. In a recent study [46], on large QM/MM calculations, authors provide a way for a rational selection of the QM region sizes for the next generation of QM/MM studies of enzymes.

Recently, hybrid methods have steadily increasing impact on the drug discovery [47–49]. In the QM/MM study of HIV-1 protease [50], the authors explored the effect of different conformations of the enzyme on its catalytic ability. Chen and co-authors [51] apply QM/MM MD simulations combining DFT and SEQM—AM1d, RM1, PM3, and PM6 methods—to study the H bonding and other interactions of inhibitors with trypsin. Their results show that the accuracy of treating the hydrogen bonding using QM/MM MD simulations of PM6 can compete with the DFT QM/MM MD simulations. Also Schirmeister et al. [52] in a study of covalent inhibitors showed that the hybrid approach was accurate enough to successfully design reversible covalent inhibitors for rhodesain. QM/MM calculations could generate electrostatic potential maps of the binding sites at QM level, thus helping to determine the protonation states of important residues and also to analyze reaction mechanisms in drug discovery targets [53]. Detailed review shows the applications of one of the most used hybrid method ONIOM including its applications for the structure-based drug design, optimization, and rescoring of docking poses or supplement for the X-ray crystallography [54].

Modern techniques add to QM/MM approach machine learning elements such as neural networks. Shen and Yang [55] put an effort to achieve the accuracy of ab initio QM/MM at the computational cost similar to SEQM/MM approaches. They developed an interesting new method and improved their previously reported QM/MM-NN (QM/MM neural network) approach with QM/MM MD simulations using an adaptive procedure.

As a future perspective and challenges, in front QM/MM MD methods in the drug design, we can point the time needed and the accuracy of these approaches. We might expect to simulate a full system at QM level in a close future. The development of both hardware and algorithms might bring quantum computers in the future to a commercial usage. Drug discovery would be a promising area of their application that will offer variety of applications [56].

3.2 Parametrization of Force Fields

Molecular mechanics force fields (FF) were developed to treat broad spectra of small organic drug-like molecules, lipids, carbohydrates, proteins, DNA, RNA, and other systems of interest. The parameters for the energy functions, in the most used FF in CADD, are derived from physical or chemical experiments and from QM calculations, usually performed at a high level of theory (pHF, DFT). The FF set of parameters includes values for different types of atoms (mass, radius, charge), chemical bonds, angles, and

dihedral angles. Experimental data used to parametrize FF can be bond lengths from X-ray and neutron diffraction, dipole moments, enthalpy of vaporization, spectroscopic parameters. Some of the best parametrized FF for small molecules that are implemented in different software for CADD are OPLS3 [57], GAFF [58], CGenFF [59], and MMFF [60]—all of them rely on a number of QM-derived parameters. Some of the recently updated FF (with QM parametrizations) for proteins include AMBER ff14sb [61], OPLS3 [57], and CHARMM [62]. Significant improvements have been achieved for the simulations of DNA with Parmbsc1, parameterized from high-level QM data [63].

DNA and RNA can form a wide variety of complex tertiary structures. In nucleic acid research, the study of structural diversity and transitions between diverse types of structures is of great importance to identify druggable RNA targets and to predict small compound binding and specificity [64]. In particular, reliable structure prediction must consider the effects of ionic phosphate groups and base pairing and stacking. Zhang and co-workers developed the AMOEBA (Atomic Multipole Optimized Energetics for Biomolecular Applications) polarizable force field for DNA and RNA, based on high-level QM calculations [65]. Molecular dynamics simulations using the AMOEBA force field were performed for 20 different DNA/RNA molecules and were compared with experimental data. The conformations were reproduced with an average RMSD below or around 2.0 Å compared to NMR structures.

3.3 Protein Structure Refinement

Structures of protein-ligand complexes obtained by X-ray crystallography are key in understanding interactions and optimizing compounds. However, crystal models still contain questionable geometric coordinates, as revealed, in particular, by the clashscore, which is the number of clashes per 1000 atoms. Errors in ligand geometry and position often lead to bad perception of the interactions with the protein, which is detrimental for compound optimization. Borbulevych et al. have developed an automated refinement process using a QM/MM based on the ONIOM method implemented in the *DivCon* package [35]. They considered 80 protein-ligand structures from the Astex diverse set. After automatic refinement, they observed an improvement in the clashscore by an average factor of 4.5, as well as improvements in Ramachandran and in rotamer outlier analyses and in ligand strain energy.

3.4 Virtual Screening (VS)

VS is essentially composed of two phases: docking and scoring. Nowadays, docking is considered reliable: the poses of docked compound into target sites are relatively well reproduced when superposed to the same compounds in co-crystallized structures. Scoring is still a problem, and the results provided by diverse scoring functions are protein-dependent [66]. To overcome this

problem, Zhou and Caflish [67] used small molecules, named probes, consisting of 2–10 atoms. Polar groups in the binding site of the protein were replaced by mimetic probes, and for each compound pose, the interaction energy value between the compound and the probes was calculated using PM6. They considered the target EphB4. First, a homology model was built using the structure of EphB2. Then 2.7 million compounds of the ZINC library, containing at least 1 hydrogen bond donor and 1 hydrogen bond acceptor, were docked into the ATP binding site, with AutoDock, resulting in ~100 million poses. Thirteen polar groups were replaced by QM probes in diverse parts of the binding site of EphB4, and cutoffs for filtering, according to QM values, were determined using four known inhibitors of EphB4. Finally, using the QM probe method, and additional filters, 23 compounds were selected for experimental validation. Three low micromolar inhibitors of EphB4 were identified.

In a recent mini-revue, Cavasotto et al. presented applications of QM methods in small molecule docking and scoring [33].

3.5 Protein-Ligand Affinity Prediction

Lu and co-workers [68] performed the computation of affinity between Akt kinase and eight diverse, selective, and potent inhibitors. They docked the eight compounds in a model of Akt, and they used the complexes for MD simulations. After, they tested two empirical scoring functions (DrugScore, DFIRE) and MM-PB/SA, and both methods found poor correlations with experimental affinity. Finally, they applied QM/MM method to optimize the complex structures, and they used QM/MM-PB/SA to calculate the interaction energies. A strong correlation appeared between computed and experimental affinities. Additionally, the QM/MM-PB/SA method was used to screen for analogues of apigenin, a potent anti-cancer compound. Four compounds were selected and tested in vitro against Akt kinase. They displayed nanomolar inhibitory activities.

To predict the binding affinity for a series of cyclin-dependent kinase 2 (CDK2) inhibitors, Mazanetz and co-workers [69] used the fragment molecular orbital (FMO) method. They considered 14 X-ray structures with 14 ligands. FMO calculations showed a good correlation to the experimental free energy of binding (r^2 of 0.68). Then, they combined the enthalpy contributions calculated by the FMO method, with entropy and solvation approximations, and they built a QSAR model. Calculated values displayed a strong correlation with experimental data (r^2 of 0.94).

The FMO method was also used to analyze docking poses of orexin-2 receptor agonists [70]. Sixteen analogues of non-peptidic OX_2R agonists were docked in a recent X-ray structure of the receptor. Two potential binding modes were observed. By using FMO, a strong correlation (r^2 of 0.87) was found between experimental values of EC_{50} and calculated values, for the "U"-shape

poses, while no significant correlation was found for the "L"-shape poses. Such findings are important for drug design of protein modulators when no co-crystal structure is available.

To illustrate the typical results obtained using FMO, we performed calculations on the complex between galectin 1 and the inhibitor thio-digalactoside (TDG) ligand, PDB entry 3OYW, Fig. 2a, and between galectin 1 and the inhibitor 3,3′-deoxy-3,3′-bis-(4-[*m*-fluorophenyl]-1*H*-1,2,3-triazol-1-yl)-thio-digalactoside (TD139), PDB entry 4Y24, Fig. 2b. While TDG has Kd = 67.3 μM for galectin 1, TD139 has Kd = 0.22 μM for the same target, thus showing ~300-fold increase in affinity compared with TDG binding [71]. The left-hand plots show the pair interaction energies (PIE) for the residues, and those on the right show the pair interaction energy decomposition analysis (PIEDA) contributions. We consider any interaction with an absolute PIE greater than or equal to 3.0 kcal/mol to be significant [72]. FMO indicated that the two inhibitors shared significant interactions with seven residues His44, Arg48, Asp54, Asn61, Trp68, Glu71, and Arg73 and one water molecule (named HOH142 in PDB entry 3OYW and named HOH 331 in PDB entry 4Y24). For the TD139 inhibitor, the FMO calculations detected additional interactions with five residues Val31, Asn46, His52, Gly53, and Asp123 and three water molecules (HOH324, 325, 328). Difference of shared interactions between TDG and TD139 complexes is shown in Fig. 2c.

3.6 Identification of Key Drivers of Protein-Ligand Binding

The heme-containing enzyme IDO1 is an attractive immunotherapy target in cancer treatment. Zou and co-workers considered a set of 20 imidazole derivatives including 4 classes of IDO1 inhibitors. The compounds were subjected to induced fit docking into the binding site of the enzyme, followed by molecular dynamics, MM/PBSA free energy calculation, and QM/MM computation with *QSite* program in Schrödinger. They discovered that Arg231 and 7-propionate of the heme group were major contributors to ligand binding, thus suggesting possible ways to improve the binding affinity of new IDO1 inhibitors [73].

3.7 Protomer/Tautomer States

To guide drug design, the correct protomer/tautomer state of binding site residues and bound molecules must be identified. X-ray crystallography is not precise enough to detect hydrogen atoms in large systems. Neutron diffraction is a unique technique that allows experimental identification of hydrogen positions in crystal structures, but is of limited use mainly due to the necessity of deuterium exchange. In a study, Borbulevych et al. applied *XModeScore* to three cases for which X-ray diffraction model and neutron diffraction model were available in the PDB database. The method involves the QM X-ray refinement of a set of structures containing all protomer/tautomer forms followed by a statistical

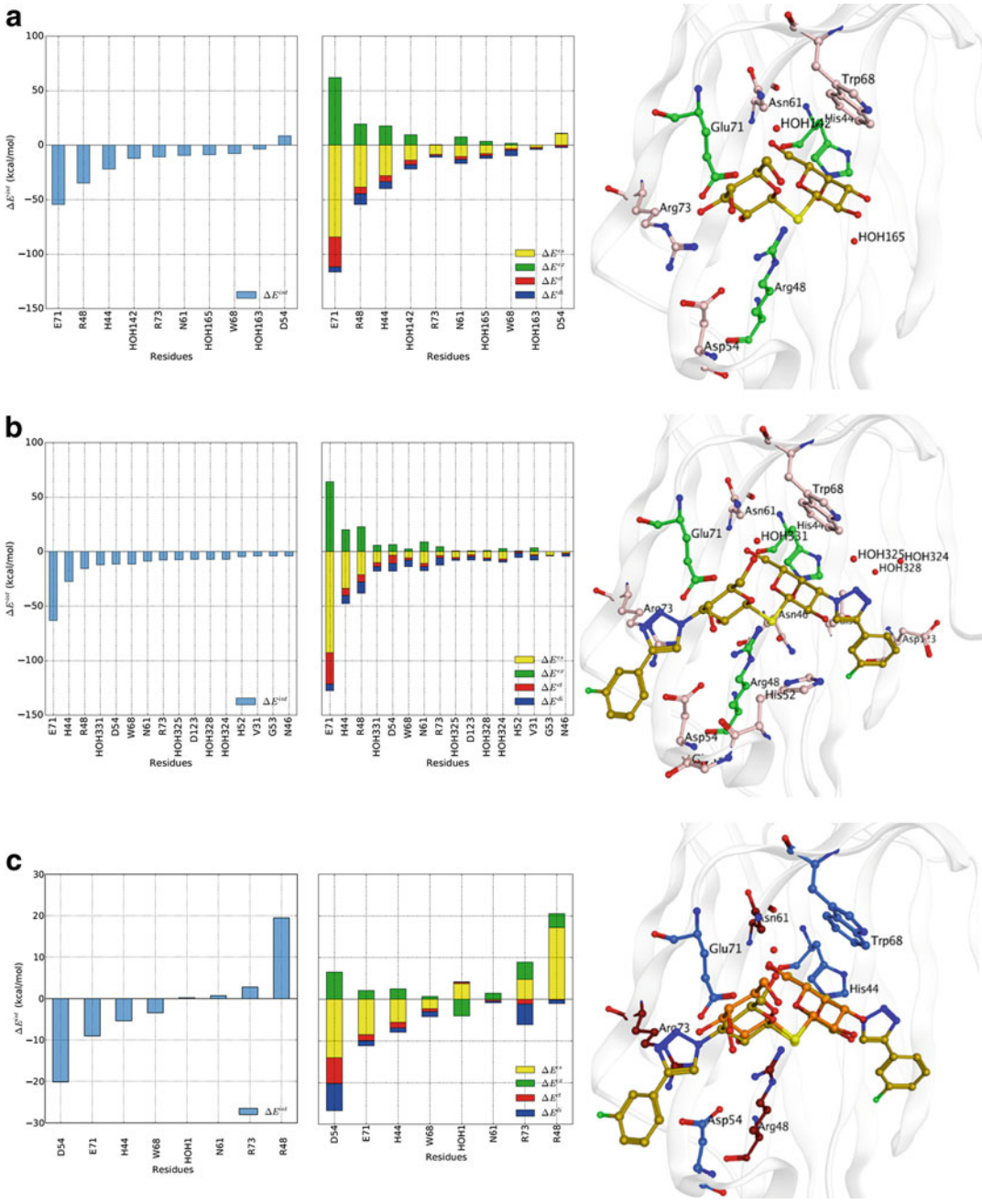

Fig. 2 FMO calculations for two galectin 1-inhibitor complexes. (**a**) Thio-digalactoside ligand (TDG), PDB entry 3OYW. (**b**) 3,3′-Deoxy-3,3′-bis-(4-[*m*-fluorophenyl]-1*H*-1,2,3-triazol-1-yl)-thio-digalactoside (TD139), PDB entry 4Y24. The left-hand plots show the total PIE for the residues, while those on the right show the PIEDA contributions. The electrostatics, exchange repulsion, charge transfer, and dispersion PIE terms are color-coded yellow, green, red, and blue, respectively. The three residues interacting more strongly with the ligands (His44, Arg48, Glu71) are shown with the carbon atoms colored in green, and the other interacting residues have their carbon atoms colored in pink. (**c**) Difference of interactions between TDG- and TD139-galectin 1 complexes. TDG is shown in orange and TD139 in gold, with the residues interacting more strongly with TD139 colored in blue and the residues interacting more strongly with TDG in dark red. The water molecules 142 and 331, in, respectively, the TDG- and the TD139-galectin 1 complexes, are at similar positions

analysis of difference electron density maps for each map candidate [74]. When applied to human carbonic anhydrase II in complex with the inhibitor acetazolamide, and to the enzyme urate oxidase in complex with uric acid monoanion, the method found the correct protomer/tautomer states of the molecules. Applied to an aspartic proteinase in complex with an inhibitor, *XModeScore* found the correct state of the catalytic aspartic acid showing protonation of the outer oxygen atom.

3.8 Cation-π and π-π Interactions

These interactions play a fundamental role in the protein-ligand binding, but they are not well described by classical force fields with fixed charge models [75]. Accurately identifying key interactions that drive the binding of β-lactam antibiotics to DD-peptidase targets, and to β-lactamase enzymes which inactivate β-lactam compounds, is essential to propose modifications to compounds in order to counter bacterial resistance. To this end, Hargis and colleagues used a combination of computational chemistry methods including quantum chemistry to analyze benzylpenicillin and a novel β-lactam peptidomimetic complexed to *Streptomyces* R61 peptidase [76]. They identified an extended π-π network for the phenyl group of benzylpenicillin with Phe120 and Trp233 that contributes into stabilizing aromatic interactions and compound efficacy for the DD-peptidase. However, structural analysis identified that this aromatic stabilization is also conserved in β-lactamases. Following their investigation, they found that interactions between the peptidomimetic tail region and the peptidase are specific when compared to interactions with class C β-lactamases. These findings suggest important modifications to β-lactam antibiotics for improving their binding and specificity.

3.9 Bioactive Conformations

The bioactive conformation of a compound is the target-bound conformation. To study the prediction of bioactive conformations using in silico approaches, Avgy-David and Senderowitz [77] have considered a set of 100 FDA-approved drugs with 1–6 rotatable bonds with available complexes in the PDB. For each compound, a large conformational ensemble was generated using three different force fields: OPLS-AA, MMFF, and CHARMm. Conformations were merged and clustered. Centroid conformations were minimized using the three force fields and four DFT methods. The probability to find the bound conformation in low-energy regions of unbound conformational ensembles was higher with QM methods and with CHARMm than with the two other force field methods.

3.10 Bi-specific Inhibitors

Restoration of p53 activity by inhibition of interaction with the two oncoproteins MDM2 and MDMX inhibits the growth of cancerous tumors in animals. Peptide and non-peptide inhibitors have been developed. They display high affinity for MDM2, but they are less efficient for inhibiting p53-MDMX interaction. To understand the

origin of such difference, Chen and co-workers [78] considered two peptide inhibitors pDI6W and pDIQ and the two oncoproteins MDM2 and MDMX. They performed MD with AMBER FF02 polarizable force field during 10 ns, followed by QM/MM-GBSA calculation. The QM region was defined by the residues forming hydrogen bonds with the inhibitors and the MM region by the rest. For the two peptides, they found better binding free energies for MDM2 than for MDMX, in accordance with experimental values. A decrease in the van der Waals interaction was the main source of the weaker binding of inhibitors to MDMX than to MDM2. Considering residue-based free energy decomposition method, and residue conformations obtained during MD, they identified M53 and Y99 in MDMX as the main origin of the weaker binding of inhibitors to MDMX than to MDM2. They concluded that the structure of future bi-specific MDM2/MDMX inhibitors should be more flexible to adapt their structure to MDMX in the identified region.

3.11 Covalent Compounds

MacDonald and Boyd explored the potential of FKBP35 in *Plasmodium falciparum* as a target for novel anti-malarial [79]. Since the enzyme contains Cys106 in the active site, they investigated where to introduce a warhead into Fk506, the natural substrate of FKBP35, to form a covalently linked inactive substrate-enzyme complex. They performed MD and QM/MM (ONIOM) calculations, and they described the transition and final states representative of the bond formation between the cysteinyl sulfur in the protein and the Michael acceptor added to carbon 41 of the substrate. Interestingly, FKBP12, a human enzyme with a highly similar active site, contains His87 at the corresponding position, suggesting a potential selective inhibition of the covalent substrate for the parasite.

3.12 Prodrugs

Six-coordinate platinum(IV) prodrugs need to be reduced to four-coordinate Pt(II) drugs in order to show activity against various cancers. Despite their important role, serious side effects limit their efficacy and motivate further studies to design next-generation Pt agents. McCormick and co-workers used electrochemical experiments and QM to decipher the mechanism for the two-electron reduction of Pt(IV) prodrugs to Pt(II) drugs [80]. They considered three Pt(IV) prodrugs. By using DFT combined with continuum solvation models, they proposed the mechanism of reduction. All three prodrugs follow a stepwise mechanism, with a metastable six-coordinate Pt(III) intermediate generated upon addition of one electron. The loss of the two axial groups present in the prodrug occurs upon addition of the second electron. A strategy to design more inert Pt(IV) prodrugs with less side effects would consist to modify the two axial groups that are lost upon reduction, in such a way that lipophilicity and ease of reduction of the prodrug are appropriately tuned.

3.13 Reaction Mechanisms

Identification of reaction mechanisms for enzymes with therapeutic interest is important for the design of specific inhibitors. Type II dehydroquinase enzymes (DHQ2) are essential enzymes for the pathogenic bacterium *Mycobacterium tuberculosis* and *Helicobacter pylori*, but MtDHQ2 and HpDHQ2 show a 50-fold difference in catalytic efficiency. To understand such difference, Lence and co-workers performed QM/MM simulations for the two enzymes and for the three reaction steps which are the generation of the catalytic tyrosinate, the formation of the enolate intermediate, and the enolate dehydration [81]. They found that the second step explains the observed differences in activity between the two enzymes, with a more efficient stabilization of the enolate intermediate by the *M. tuberculosis* enzyme. Comparing the two enzymes, they found differences for a water molecule in the catalytic pocket and for the flexibility of the substrate-covering loop. The loop has limited flexibility for HpDHQ2, due to a salt bridge between two residues in this loop, while its flexibility is higher for MtDHQ2 due to an apolar residue in one of the corresponding positions. Crystal structures of DHQ2-ligand complexes exist, but they show a highly similar binding mode for both enzymes, while the inhibitors present in these structures have different inhibitory potencies. Deciphering enzymatic mechanisms and differences in enzyme reaction steps of different species is essential for the rational design of more efficient chemical entities.

3.14 Drug Metabolism

Drug metabolism has a strong impact on clearance and toxicity. Structures for main cytochrome P450 have been identified, and thus structure-based drug metabolism can be considered. In an early work, the metabolism of sirolimus, and its derivative everolimus, was investigated by Kuhn and co-workers [82]. They used a process in three steps: first, the compounds were docked into the active site of CYP3A4, then molecular dynamics calculations were performed, and finally the enzyme-substrate interactions were calculated using QM. Predictions of the regiospecificities of the hydroxylations and O-dealkylations for the two substrates were in good agreement with experimental data. They also identified substrate/CYP interactions that are important for the metabolism of the substrate, and they explained why the metabolism in everolimus is reduced compared to sirolimus. Many CYP isoforms show high levels of flexibility and can bind a wide variety of ligands. Therefore induced fit docking of compounds followed by MD and QM calculations help in incorporating the CYP flexibility in the structure-based process [83].

Recently Tyzack and Kirchmair have reviewed diverse approaches and software packages for drug metabolism predictions, including ligand-based approaches and methods for metabolite structure prediction [84].

3.15 QSAR Models

Golgi α-mannosidase II (GMII) is a Zn^{2+} co-factor-dependent glycoside hydrolase, and lysosomal α-mannosidase (LMAN) is a protein with a closely related active site. GMII inhibitors have anti-tumor activity, but inhibition of LMAN is not wanted. As all known potent inhibitors of GMII also show inhibition for LMAN, Bobovská and colleagues have built QSAR models to accurately predict the affinity of compounds for both targets [85]. They docked 57 inhibitors and 25 non-active compounds on the 2 protein sites, and they employed a combination of interaction energy descriptors computed using empirical and QM approaches. Using 5 and 7 descriptors, they achieved RMSD of 0.8 and 1.1 kcal/mol for ΔG_{bind} for, respectively, GMII and LMAN, which is enough to predict selectivity.

3.16 Molecular Quantum Similarity

Ligand-based virtual screening (LBVS) was performed by Sullivan and co-workers, using electron density attributes of chemical compounds computed at the quantum level. They described compounds by combining DFT and topological theory of atoms in molecules (AIM). Quantum similarity was calculated between known inhibitors and compounds in commercial databases, and compounds were selected without explicit reference to chemical structures. The method, applied to LBVS of anti-malarial agents, discovered new anti-malarial compounds which are chemically dissimilar, but show similarity at the quantum level [86, 87].

3.17 Enzyme Design

The design of artificial enzymes, in biotechnology and biochemistry, requires the understanding of transition states and the quantification of subtle effects due to small modifications introduced to the proteins [88]. The 34E4 catalytic antibody which catalyzes Kemp elimination of 5-nitrobenzisoxazole, as well as its Glu50Asp variant which shows a 30-fold reduction in the catalytic performance, was considered by Alexandrova and Jorgensen [89]. They used QM/MM Monte Carlo simulations and free energy perturbation theory to elucidate the mechanism of Kemp elimination catalyzed by 34E4. Glu50 is the key residue in 34E4, and substitution by Asp50 resulted in the increase of the computed activation barrier by 2.4 kcal/mol, which corresponds to a 62-fold reduction in the reaction rate at 25 °C, in good agreement with experimental data.

4 Conclusion and Outlook

QM methods provide high accuracy in the description of receptor-ligand interactions, the estimation of binding affinities, and the modeling of bond formation or breakage. They model electronic polarization, charge transfer, halogen bonding, and metal coordination, at the expense of long computing time. For complex biological systems, hybrid QM/MM approaches, which combine the accuracy of QM with the speed of calculation of MM, are used to make the most of both methods.

In early stages of drug discovery, QM methods contribute to refine X-ray structures of active sites of proteins for virtual screening, and for electronically complex binding sites, to estimate the affinity of small lists of docked compounds. In the subsequent optimization phases, QM methods are particularly important to predict the nature and the relative binding affinity of compounds to targets, mutated targets, and off-targets, in order to select the best compounds with a given selectivity profile, for synthesis and testing. QM is particularly needed for metal-containing binding site systems, for aromatic-containing compounds, for the identification of protomeric and tautomeric states, and for the study and design of covalent compounds and prodrugs. It opens the way to investigate reaction mechanisms, decipher substrate-enzyme transition states, and predict drug metabolism. QM is also key for parameterization of force fields regarding new types of targets, as DNA/RNA, and for providing QM descriptors for improved QSAR/QSPR models.

Today, QM methods are an unavoidable part of the CADD toolbox, driven by advanced algorithms and unprecedented computational power.

Acknowledgments

The authors thank Christophe Iftner, Franck Taillez, and Emilie Pihan (Evotec (France) SAS, Toulouse, France) for valuable suggestions to the manuscript.

References

1. Szabo A, Ostlund NS (1996) Modern quantum chemistry. Dover Publishing, Mineola, NY
2. Cramer CJ (2006) Essentials of computational chemistry: theories and models. Wiley, Chichester, UK
3. Jensen F (2007) Introduction to computational chemistry. Wiley, Chichester, UK
4. Pople JA, Beveridge DL (1970) Approximate molecular orbital theory. McGraw-Hill, New York
5. Dewar MJS, Zoebisch EG, Healy EF, Stewart JJP (1985) AM1: a new general purpose quantum mechanical molecular model. J Am Chem Soc 107:3902–3909. https://doi.org/10.1021/ja00299a024
6. Stewart JJP (1989) Optimization of parameters for semiempirical methods I. Method. J Comput Chem 10:209–220. https://doi.org/10.1002/jcc.540100208
7. Dewar MJS, Jie C, Yu J (1993) SAM1; the first of a new series of general purpose quantum mechanical molecular models. Tetrahedron 49:5003–5038. https://doi.org/10.1016/S0040-4020(01)81868-8
8. Repasky MP, Chandrasekhar J, Jorgensen WL (2002) PDDG/PM3 and PDDG/MNDO: improved semiempirical methods. J Comput Chem 23:1601–1622. https://doi.org/10.1002/jcc.10162
9. Stewart JJ (2007) Optimization of parameters for semiempirical methods V: modification of NDDO approximations and application to 70 elements. J Mol Model 13:1173–1213. https://doi.org/10.1007/s00894-007-0233-4
10. Řezáč J, Fanfrlík J, Salahub D, Hobza P (2009) Semiempirical quantum chemical PM6 method augmented by dispersion and H-bonding correction terms reliably describes

various types of noncovalent complexes. J Chem Theory Comput 5:1749–1760. https://doi.org/10.1021/ct9000922

11. Dral PO, Wu X, Spörkel L, Koslowski A, Weber W, Steiger R, Scholten M, Thiel W (2016) Semiempirical quantum-chemical orthogonalization-corrected methods: theory, implementation, and parameters. J Chem Theory Comput 12:1082–1096. https://doi.org/10.1021/acs.jctc.5b01046
12. Dral PO, Wu X, Thiel W (2019) Semiempirical quantum-chemical methods with orthogonalization and dispersion corrections. J Chem Theory Comput 15:1743–1760. https://doi.org/10.1021/acs.jctc.8b01265
13. Kříž K, Řezáč J (2019) Reparametrization of the COSMO solvent model for semiempirical methods PM6 and PM7. J Chem Inf Model 59:229–235. https://doi.org/10.1021/acs.jcim.8b00681
14. Hehre WJ, Ditchfield R, Pople JA (1972) Self-consistent molecular orbital methods. 12. Further extensions of Gaussian-type basis sets for use in molecular-orbital studies of organic-molecules. J Chem Phys 56:2257. https://doi.org/10.1063/1.1677527
15. Jensen F (2013) Atomic orbital basis sets. WIREs Comput Mol Sci 3:273–295. https://doi.org/10.1002/wcms.1123
16. Dunning TH (1989) Gaussian basis sets for use in correlated molecular calculations. I. The atoms boron through neon and hydrogen. J Chem Phys 90:1007–1023. https://doi.org/10.1063/1.456153
17. Kendall RA, Dunning TH, Harrison RJ (1992) Electron affinities of the first-row atoms revisited. Systematic basis sets and wave functions. J Chem Phys 96:6796–6806. https://doi.org/10.1063/1.462569
18. Weigend F, Ahlrichs R (2005) Balanced basis sets of split valence, triple zeta valence and quadruple zeta valence quality for H to Rn: design and assessment of accuracy. Phys Chem Chem Phys 7:3297–3305. https://doi.org/10.1039/b508541a
19. Møller C, Plesset MS (1934) Note on an approximation treatment for many-electron systems. Phys Rev 46:618–622. https://doi.org/10.1103/PhysRev.46.618
20. Shavitt I, Bartlett RJ (2009) Many-body methods in chemistry and physics: MBPT and coupled-cluster theory. Cambridge University Press, Cambridge
21. Ramabhadran RO, Raghavachari K (2013) Extrapolation to the gold-standard in quantum chemistry: computationally efficient and accurate CCSD(T) energies for large molecules using an automated thermochemical hierarchy. J Chem Theory Comput 9:3986–3994. https://doi.org/10.1021/ct400465q
22. Hohenberg P, Kohn W (1964) Inhomogeneous electron gas. Phys Rev 136: B864–B871
23. Kohn W, Sham LJ (1965) Self-consistent equations including exchange and correlation effects. Phys Rev 140:A1133–A1138. https://doi.org/10.1103/PhysRev.140.A1133
24. Perdew JP (1986) Density-functional approximation for the correlation energy of the inhomogeneous electron gas. Phys Rev B Condens Matter 33:8822–8824. https://doi.org/10.1103/physrevb.33.8822
25. Lee CT, Yang WT, Parr RG (1988) Development of the Colle-Salvetti correlation-energy formula into a functional of the electron density. Phys Rev B Condens Matter Mater Phys 37:785–789. https://doi.org/10.1103/PhysRevB.37.785
26. Becke AD (1993) Density-functional thermochemistry. III. The role of exact exchange. J Chem Phys 98:5648–5652. https://doi.org/10.1063/1.464913
27. Perdew JP, Burke K, Ernzerhof M (1996) Generalized gradient approximation made simple. Phys Rev Lett 77:3865–3868. https://doi.org/10.1103/PhysRevLett.77.3865
28. Zhao Y, Truhlar DG (2008) The M06 suite of density functionals for main group thermochemistry, thermochemical kinetics, noncovalent interactions, excited states, and transition elements: two new functionals and systematic testing of four M06-class functionals and 12 other functionals. Theor Chem Accounts 120:215–241. https://doi.org/10.1007/s00214-007-0310-x
29. Liao C, Sitzmann M, Pugliese A, Nicklaus MC (2011) Software and resources for computational medicinal chemistry. Future Med Chem 3(8):1057–1085. https://doi.org/10.4155/fmc.11.63
30. Kitchen DB (2017) Computer-aided drug discovery research at a global contract research organization. J Comput Aided Mol Des 31(3):309–318. https://doi.org/10.1007/s10822-016-9991-3
31. Muegge I, Bergner A, Kriegl JM (2017) Computer-aided drug design at Boehringer Ingelheim. J Comput Aided Mol Des 31 (3):275–285. https://doi.org/10.1007/s10822-016-9975-3

32. Nitsche MA, Ferreria M, Mocskos EE, González Lebrero MC (2014) GPU accelerated implementation of density functional theory for hybrid QM/MM simulations. J Chem Theory Comput 10(3):959–967. https://doi.org/10.1021/ct400308n
33. Cavasotto CN, Adler NS, Aucar MG (2018) Quantum chemical approaches in structure-based virtual screening and lead optimization. Front Chem 6:188. https://doi.org/10.3389/fchem.2018.00188
34. Shi M, Xu D, Zeng J (2018) GPU accelerated quantum virtual screening: application for the natural inhibitors of New Delhi metalloprotein (NDM-1). Front Chem 6:564. https://doi.org/10.3389/fchem.2018.00564
35. Borbulevych O, Martin RI, Westerhoff LM (2018) High-throughput quantum-mechanics/molecular-mechanics (ONIOM) macromolecular crystallographic refinement with PHENIX/DivCon: the impact of mixed Hamiltonian methods on ligand and protein structure. Acta Cryst D74:1063–1077. https://doi.org/10.1107/S2059798318012913
36. Rode BM, Hofer TS, Randolf BR, Schwenk CF, Xenides D, Vchirawongkwin V (2006) Ab initio quantum mechanical charge field (QMCF) molecular dynamics: a QM/MM – MD procedure for accurate simulations of ions and complexes. Theor Chem Accounts 115:77–85. https://doi.org/10.1007/s00214-005-0049-1
37. Senn HM, Thiel W (2009) QM/MM methods for biomolecular systems. Angew Chem Int Ed Engl 48(7):1198–1229. https://doi.org/10.1002/anie.200802019
38. Cornell WD, Cieplak P, Bayly CI, Kollman PA (1993) Application of RESP charges to calculate conformational energies, hydrogen bond energies, and free energies of solvation. J Am Chem Soc 115:9620–9631. https://doi.org/10.1021/ja00074a030
39. Kotev M, Pascual R, Almansa C, Guallar V, Soliva R (2018) Pushing the limits of computational structure-based drug design with a cryo-EM structure: the Ca^{2+} channel α2δ-1 subunit as a test case. J Chem Inf Model 58(8):1707–1715. https://doi.org/10.1021/acs.jcim.8b00347
40. Bekker GJ, Araki M, Oshima K, Okuno Y, Kamiya N (2019) Dynamic docking of a medium-sized molecule to its receptor by multicanonical MD simulations. J Phys Chem B 123(11):2479–2490. https://doi.org/10.1021/acs.jpcb.8b12419
41. Wang J, Zhao C, Tu J, Yang H, Zhang X, Lv W, Zhai H (2019) Design of novel quinoline-aminopiperidine derivatives as Mycobacterium tuberculosis (MTB) GyrB inhibitors: an in silico study. J Biomol Struct Dyn 37(11):2913–2925. https://doi.org/10.1080/07391102.2018.1498806
42. Ryde U, Söderhjelm P (2016) Ligand-binding affinity estimates supported by quantum-mechanical methods. Chem Rev 116(9):5520–5566. https://doi.org/10.1021/acs.chemrev.5b00630
43. Arodola OA, Soliman ME (2017) Quantum mechanics implementation in drug-design workflows: does it really help? Drug Des Devel Ther 11:2551–2564. https://doi.org/10.2147/DDDT.S126344
44. Ganesan A, Coote ML, Barakat K (2017) Molecular dynamics-driven drug discovery: leaping forward with confidence. Drug Discov Today 22(2):249–269. https://doi.org/10.1016/j.drudis.2016.11.001
45. Awoonor-Williams E, Walsh AG, Rowley CN (2017) Modeling covalent-modifier drugs. Biochim Biophys Acta Proteins Proteom 1865(11 Pt B):1664–1675. https://doi.org/10.1016/j.bbapap.2017.05.009
46. Kulik HJ, Zhang J, Klinman JP, Martínez TJ (2016) How large should the QM region be in QM/MM calculations? The case of catechol O-methyltransferase. J Phys Chem B 120(44):11381–11394. https://doi.org/10.1021/acs.jpcb.6b07814
47. Lodola A, De Vivo M (2012) The increasing role of QM/MM in drug discovery. Adv Protein Chem Struct Biol 87:337–362. https://doi.org/10.1016/B978-0-12-398312-1.00011-1
48. Barbault F, Maurel F (2015) Simulation with quantum mechanics/molecular mechanics for drug discovery. Expert Opin Drug Discov 10(10):1047–1057. https://doi.org/10.1517/17460441.2015.1076389
49. Nascimento ÉCM, Oliva M, Świderek K, Martins JBL, Andrés J (2017) Binding analysis of some classical acetylcholinesterase inhibitors: insights for a rational design using free energy perturbation method calculations with QM/MM MD simulations. J Chem Inf Model 57(4):958–976. https://doi.org/10.1021/acs.jcim.7b00037
50. Ribeiro AJM, Santos-Martins D, Russo N, Ramos MJ, Fernandes PA (2015) Enzymatic flexibility and reaction rate: a QM/MM study of HIV-1 protease. ACS Catal 5:5617–5626. https://doi.org/10.1021/acscatal.5b00759
51. Chen J, Wang J, Zhang Q, Chen K, Zhu W (2015) A comparative study of trypsin specificity based on QM/MM molecular dynamics simulation and QM/MM GBSA calculation. J Biomol Struct Dyn 33(12):2606–2618.

https://doi.org/10.1080/07391102.2014.1003146

52. Schirmeister T, Kesselring J, Jung S, Schneider TH, Weickert A, Becker J, Lee W, Bamberger D, Wich PR, Distler U, Tenzer S, Johé P, Hellmich UA, Engels B (2016) Quantum chemical-based protocol for the rational design of covalent inhibitors. J Am Chem Soc 138(27):8332–8335. https://doi.org/10.1021/jacs.6b03052
53. Cavalli A, Carloni P, Recanatini M (2006) Target-related applications of first principles quantum chemical methods in drug design. Chem Rev 106(9):3497–3519. https://doi.org/10.1021/cr050579p
54. Chung LW, Sameera WM, Ramozzi R, Page AJ, Hatanaka M, Petrova GP, Harris TV, Li X, Ke Z, Liu F, Li HB, Ding L, Morokuma K (2015) The ONIOM method and its applications. Chem Rev 115(12):5678–5796. https://doi.org/10.1021/cr5004419
55. Shen L, Yang W (2018) Molecular dynamics simulations with quantum mechanics/molecular mechanics and adaptive neural networks. J Chem Theory Comput 14(3):1442–1455. https://doi.org/10.1021/acs.jctc.7b01195
56. Cao Y, Romero J, Aspuru-Guzik A (2018) Potential of quantum computing for drug discovery. IBM J Res Dev 62(6):1–6. https://doi.org/10.1147/JRD.2018.2888987
57. Harder E, Damm W, Maple J, Wu C, Reboul M, Xiang JY, Wang L, Lupyan D, Dahlgren MK, Knight JL, Kaus JW, Cerutti DS, Krilov G, Jorgensen WL, Abel R, Friesner RA (2016) OPLS3: a force field providing broad coverage of drug-like small molecules and proteins. J Chem Theory Comput 12:281–296. https://doi.org/10.1021/acs.jctc.5b00864
58. Wang J, Wolf RM, Caldwell JW, Kollman PA, Case DA (2004) Development and testing of a general AMBER force field. J Comput Chem 25:1157–1174. https://doi.org/10.1002/jcc.20035
59. Vanommeslaeghe K, Hatcher E, Acharya C, Kundu S, Zhong S, Shim J, Darian E, Guvench O, Lopes P, Vorobyov I, Mackerell AD Jr (2010) CHARMM general force field: a force field for drug-like molecules compatible with the CHARMM all-atom additive biological force fields. J Comput Chem 31:671–690. https://doi.org/10.1002/jcc.21367
60. Halgren TA (1999) MMFF VI. MMFF94s option for energy minimization studies. J Comput Chem 20:720–729. https://doi.org/10.1002/(SICI)1096-987X(199905)20:73.0.CO;2-X
61. Maier JA, Martinez C, Kasavajhala K, Wickstrom L, Hauser KE, Simmerling C (2015) ff14SB: improving the accuracy of protein side chain and backbone parameters from ff99SB. J Chem Theory Comput 11:3696–3713. https://doi.org/10.1021/acs.jctc.5b00255
62. Brooks BR, Brooks CL III, Mackerell AD Jr, Nilsson L, Petrella RJ, Roux B, Won Y, Archontis G, Bartels C, Boresch S, Caflisch A, Caves L, Cui Q, Dinner AR, Feig M, Fischer S, Gao J, Hodoscek M, Im W, Kuczera K, Lazaridis T, Ma J, Ovchinnikov V, Paci E, Pastor RW, Post CB, Pu JZ, Schaefer M, Tidor B, Venable RM, Woodcock HL, Wu X, Yang W, York DM, Karplus M (2009) CHARMM: the biomolecular simulation program. J Comput Chem 30:1545–1614. https://doi.org/10.1002/jcc.21287
63. Ivani I, Dans PD, Noy A, Pérez A, Faustino I, Hospital A, Walther J, Andrio P, Goñi R, Balaceanu A, Portella G, Battistini F, Gelpí JL, González C, Vendruscolo M, Laughton CA, Harris SA, Case DA, Orozco M (2016) Parmbsc1: a refined force field for DNA simulations. Nat Methods 13:55–58. https://doi.org/10.1038/nmeth.3658
64. Sztuba-Solinska J, Chavez-Calvillo G, Cline SE (2019) Unveiling the druggable RNA targets and small molecule therapeutics. Bioorg Med Chem 27(10):2149–2165. https://doi.org/10.1016/j.bmc.2019.03.057
65. Zhang C, Lu C, Jing Z, Wu C, Piquemal JP, Ponder JW, Ren P (2018) AMOEBA polarizable atomic multipole force field for nucleic acids. J Chem Theory Comput 14(4):2084–2108. https://doi.org/10.1021/acs.jctc.7b01169
66. Li Y, Liu Z, Li J, Han L, Liu J, Zhao Z, Wang R (2014) Comparative assessment of scoring functions on an updated benchmark: 2. Evaluation methods and general results. J Chem Inf Model 54(6):1700–1716. https://doi.org/10.1021/ci500080q
67. Zhou T, Caflish A (2010) High-throughput virtual screening using quantum mechanical probes: discovery of selective kinase inhibitors. ChemMedChem 5(7):1007–1014. https://doi.org/10.1002/cmdc.201000085
68. Lu J, Zhang Z, Ni Z, Shen H, Tu Z, Liu H, Lu R (2014) QM/MM-PB/SA scoring of the interaction strength between Akt kinase and apigenin analogues. Comput Biol Chem 52:25–33. https://doi.org/10.1016/j.compbiolchem.2014.07.002
69. Mazanetz MP, Ichihara O, Law RJ, Whittaker M (2011) Prediction of cyclin-dependent kinase 2 inhibitor potency using the fragment

molecular orbital method. J Chem 3:2. https://doi.org/10.1186/1758-2946-3-2

70. Heifetz A, Aldeghi M, Chudyk EI, Fedorov DG, Bodkin MJ, Biggin PC (2016) Using the fragment molecular orbital method to investigate agonist-orexin-2 receptor interactions. Biochem Soc Trans 44(2):574–581. https://doi.org/10.1042/BST20150250
71. Hsieh TJ, Lin HY, Tu Z, Lin TC, Wu SC, Tseng YY, Liu FT, Hsu ST, Lin CH (2016) Dual thio-digalactoside-binding modes of human galectins as the structural basis for the design of potent and selective inhibitors. Scientific Rep 6:29457. https://doi.org/10.1038/srep29457
72. Chudyk EI, Sarrat L, Aldeghi M, Fedorov DG, Bodkin MJ, James T, Southey M, Robinson R, Morao I, Heifetz A (2018) Exploring GPCR-ligand interactions with the Fragment Molecular Orbital (FMO) method. Methods Mol Biol 1705:179–195. https://doi.org/10.1007/978-1-4939-7465-8_8
73. Zou Y, Wang F, Wang Y, Guo W, Zhang Y, Xu Q, Lai Y (2017) Systematic study of imidazoles inhibiting IDO1 via the integration of molecular mechanics and quantum mechanics calculations. Eur J Med Chem 131:152–170. https://doi.org/10.1016/j.ejmech.2017.03.021
74. Borbulevych O, Martin RI, Tickle IJ, Westerhoff LM (2016) XModeScore: a novel method for accurate protonation/tautomer-state determination using quantum-mechanically driven macromolecular X-ray crystallographic refinement. Acta Cryst D72:586–598. https://doi.org/10.1107/S2059798316002837
75. Zhou T, Huang D, Caflisch A (2010) Quantum mechanical methods for drug design. Curr Top Med Chem 10(1):33–45. https://doi.org/10.2174/156802610790232242
76. Hargis JC, Vankayala SL, White JK, Woodcock HL (2014) Identification and characterization of noncovalent interactions that drive binding and specificity in DD-peptidases and β-lactamases. J Chem Theory Comput 10(2):855–864. https://doi.org/10.1021/ct400968v
77. Avgy-David HH, Senderowitz H (2015) Toward focusing conformational ensembles on bioactive conformations: a molecular mechanics/quantum mechanics study. J Chem Inf Model 55:2154–2167. https://doi.org/10.1021/acs.jcim.5b00259
78. Chen J, Wang J, Zhang Q, Chen K, Zhu W (2015) Probing origin of binding difference of inhibitors to MDM2 and MDMX by polarizable molecular dynamics simulation and QM/MM-GBSA calculation. Sci Rep 5:17421. https://doi.org/10.1038/srep17421
79. MacDonald CA, Boyd RJ (2015) Computational insights into the suicide inhibition of Plasmodium falciparum Fk506-binding protein 35. Bioorg Med Chem Lett 25(16):3221–3225. https://doi.org/10.1016/j.bmcl.2015.05.079
80. McCormick MC, Keijzer K, Polavarapu A, Schultz FA, Baik MH (2014) Understanding intrinsically irreversible, non-Nernstian, two-electron redox processes: a combined experimental and computational study of the electrochemical activation of platinum (IV) antitumor prodrugs. J Am Chem Soc 136(25):8992–9000. https://doi.org/10.1021/ja5029765
81. Lence E, van der Kamp MW, González-Bello C, Mulholland AJ (2018) QM/MM simulations identify the determinants of catalytic activity differences between type II dehydroquinase enzymes. Org Biomol Chem 16(24):4443–4455. https://doi.org/10.1039/c8ob00066b
82. Kuhn B, Jacobsen W, Christians U, Benet LZ, Kollman PA (2001) Metabolism of sirolimus and its derivative everolimus by cytochrome P450 3A4: insights from docking, molecular dynamics, and quantum chemical calculations. J Med Chem 44(12):2027–2034. https://doi.org/10.1021/jm010079y
83. Sun H, Scott DO (2010) Structure-based drug metabolism predictions for drug design. Chem Biol Drug Des 75:3–17. https://doi.org/10.1111/j.1747-0285.2009.00899.x
84. Tyzack JD, Kirchmair J (2019) Computational methods and tools to predict cytochrome P450 metabolism for drug discovery. Chem Biol Drug Des 93(4):377–386. https://doi.org/10.1111/cbdd.13445
85. Bobovská A, Tvaroška I, Kóňa J (2016) Using DFT methodology for more reliable predictive models: design of inhibitors of Golgi α-mannosidase II. J Mol Graph Model 66:47–57. https://doi.org/10.1016/j.jmgm.2016.03.004
86. Sullivan DJ Jr, Kaludov N, Martinov MN (2011) Discovery of potent, novel, non-toxic anti-malarial compounds via quantum modelling, virtual screening and in vitro experimental validation. Malar J 10:274. https://doi.org/10.1186/1475-2875-10-274
87. Sullivan DJ, Liu Y, Mott BT, Kaludov N, Martinov MN (2015) Discovery of novel liver-stage antimalarials through quantum

similarity. PLoS One 10(5):e0125593. https://doi.org/10.1371/journal.pone.0125593

88. Świderek K, Tuñón I, Moliner V, Bertran J (2015) Computational strategies for the design of new enzymatic functions. Arch Biochem Biophys 582:68–79. https://doi.org/10.1016/j.abb.2015.03.013
89. Alexandrova AN, Jorgensen WL (2009) Origin of the activity drop with the E50D variant of catalytic antibody 34E4 for Kemp elimination. J Phys Chem B 113(2):497–504. https://doi.org/10.1021/jp8076084
90. Gong W, Wu R, Zhang Y (2015) Thiol versus hydroxamate as zinc binding group in HDAC inhibition: an ab initio QM/MM molecular dynamics study. J Comput Chem 36:2228–2235. https://doi.org/10.1002/jcc.24203
91. Hitzenberger M, Schuster D, Hofer TS (2017) The binding mode of the sonic hedgehog inhibitor robotnikinin, a combined docking and QM/MM MD study. Front Chem 5:76. https://doi.org/10.3389/fchem.2017.00076
92. Steinmann C, Olsson MA, Ryde U (2018) Relative ligand-binding free energies calculated from multiple short QM/MM MD simulations. J Chem Theory Comput 14:3228–3237. https://doi.org/10.1021/acs.jctc.8b00081
93. Zhu T, Xiao X, Ji C, Zhang JZ (2013) A new quantum calibrated force field for zinc-protein complex. J Chem Theory Comput 9(3):1788–1798. https://doi.org/10.1021/ct301091z
94. Xiong X, Chen Z, Cossins BP, Xu Z, Shao Q, Ding K, Zhu W, Shi J (2015) Force fields and scoring functions for carbohydrate simulation. Carbohydr Res 401:73–81. https://doi.org/10.1016/j.carres.2014.10.028
95. Cole DJ, Vilseck JZ, Tirado-Rives J, Payne MC, Jorgensen WL (2016) Biomolecular force field parameterization via atoms-in-molecule electron density partitioning. J Chem Theory Comput 12(5):2312–2323. https://doi.org/10.1021%2Facs.jctc.6b00027
96. Visscher KM, Geerke DP (2019) Deriving force-field parameters from first principles using a polarizable and higher order dispersion model. J Chem Theory Comput 15(3):1875–1883. https://doi.org/10.1021/acs.jctc.8b01105
97. Hsiao YW, Sanchez-Garcia E, Doerr M, Thiel W (2010) Quantum refinement of protein structures: implementation and application to the red fluorescent protein DsRed.M1. J Phys Chem B 114(46):15413–15423. https://doi.org/10.1021/jp108095n
98. Li X, Hayik SA, Merz KM Jr (2010) QM/MM X-ray refinement of zinc metalloenzymes. J Inorg Biochem 104(5):512–522. https://doi.org/10.1016/j.jinorgbio.2009.12.022
99. Fu Z, Li X, Miao Y, Merz KM Jr (2013) Conformational analysis and parallel QM/MM X-ray refinement of protein bound anti-Alzheimer drug donepezil. J Chem Theory Comput 9(3):1686–1693. https://doi.org/10.1021/ct300957x
100. Dittrich B, Lübben J, Mebs S, Wagner A, Luger P, Flaig R (2017) Accurate bond lengths to hydrogen atoms from single-crystal X-ray diffraction by including estimated hydrogen ADPs and comparison to neutron and QM/MM benchmarks. Chemistry 23(19):4605–4614. https://doi.org/10.1002/chem.201604705
101. Chaskar P, Zoete V, Röhrig UF (2014) Toward on-the-fly quantum mechanical/molecular mechanical (QM/MM) docking: development and benchmark of a scoring function. J Chem Inf Model 54(11):3137–3152. https://doi.org/10.1021/ci5004152
102. Wichapong K, Rohe A, Platzer C, Slynko I, Erdmann F, Schmidt M, Sippl W (2014) Application of docking and QM/MM-GBSA rescoring to screen for novel Myt1 kinase inhibitors. J Chem Inf Model 54(3):881–893. https://doi.org/10.1021/ci4007326
103. Zang P, Gong A, Zhang P, Yu J (2016) Targeting druggable enzymome by exploiting natural medicines: an in silico-in vitro integrated approach to combating multidrug resistance in bacterial infection. Pharm Biol 54(4):604–618. https://doi.org/10.3109/13880209.2015.1068338
104. Khandelwal A, Balaz S (2007) QM/MM linear response method distinguishes ligand affinities for closely related metalloproteins. Proteins 69(2):326–339. https://doi.org/10.1002/prot.21500
105. Sawada T, Fedorov DG, Kitaura K (2010) Role of the key mutation in the selective binding of avian and human influenza hemagglutinin to sialosides revealed by quantum-mechanical calculations. J Am Chem Soc 132(47):16862–16872. https://doi.org/10.1021/ja105051e
106. Rathore RS, Sumakanth M, Reddy MS, Reddanna P, Rao AA, Erion MD, Reddy MR (2013) Advances in binding free energies calculations: QM/MM-based free energy perturbation method for drug design. Curr Pharm Des 19(26):4674–4686. https://doi.org/10.2174/1381612811319260002

107. Otsuka T, Okimoto N, Taiji M (2015) Assessment and acceleration of binding energy calculations for protein-ligand complexes by the fragment molecular orbital method. J Comput Chem 36(30):2209–2218. https://doi.org/10.1002/jcc.24055
108. Su PC, Tsai CC, Mehboob S, Hevener KE, Johnson ME (2015) Comparison of radii sets, entropy, QM methods, and sampling on MM-PBSA, MM-GBSA, and QM/MM-GBSA ligand binding energies of *F. tularensis* Enoyl-ACP reductase (FabI). J Comput Chem 36(25):1859–1873. https://doi.org/10.1002/jcc.24011
109. Ehrlich S, Göller AH, Grimme S (2017) Towards full quantum-mechanics-based protein-ligand binding affinities. ChemPhysChem 18(8):898–905. https://doi.org/10.1002/cphc.201700082
110. Caballero J, Alzate-Morales JH, Vergara-Jaque A (2011) Investigation of the differences in activity between hydroxycycloalkyl N1 substituted pyrazole derivatives as inhibitors of B-Raf kinase by using docking, molecular dynamics, QM/MM, and fragment-based de novo design: study of binding mode of diastereomer compounds. J Chem Inf Model 51(11):2920–2931. https://doi.org/10.1021/ci200306w
111. Sun TY, Wang Q, Zhang J, Wu T, Zhang F (2013) Trastuzumab-Peptide interactions: mechanism and application in structure-based ligand design. Int J Mol Sci 14 (8):16836–16850. https://doi.org/10.3390/ijms140816836
112. De Colibus L, Wang X, Spyrou JAB, Kelly J, Ren J, Grimes J, Puerstinger G, Stonehouse N, Walter TS, Hu Z, Wang J, Li X, Peng W, Rowlands D, Fry EE, Rao Z, Stuart DI (2014) More powerful virus inhibitors from structure-based analysis of HEV71 capsid-binding molecules. Nat Struct Mol Biol 21(3):282–288. https://doi.org/10.1038/nsmb.2769
113. Zanatta G, Nunes G, Bezerra EM, da Costa RF, Martins A, Caetano EW, Freire VN, Gottfried C (2014) Antipsychotic haloperidol binding to the human dopamine D3 receptor: beyond docking through QM/MM refinement toward the design of improved schizophrenia medicines. ACS Chem Neurosci 5 (10):1041–1054. https://doi.org/10.1021/cn500111e
114. Yu N, Hayik SA, Wang B, Liao N, Reynolds CH, Merz KM Jr (2006) Assigning the protonation states of the key aspartates in β-Secretase using QM/MM X-ray structure refinement. J Chem Theory Comput 2 (4):1057–1069. https://doi.org/10.1021/ct0600060
115. Lee W, Luckner SR, Kisker C, Tonge PJ, Engels B (2011) Elucidation of the protonation states of the catalytic residues in *mt*KasA - implications for inhibitor design. Biochemistry 50(25):5743–5756. https://doi.org/10.1021/bi200006t
116. Vega-Teijido MA, El Chamy Maluf S, Bonturi CR, Sambrano JR, Ventura ON (2014) Theoretical insight into the mechanism for the inhibition of the cysteine protease cathepsin B by 1,2,4-thiadiazole derivatives. J Mol Model 20(6):2254. https://doi.org/10.1007/s00894-014-2254-0
117. Ma S, Vogt KA, Petrillo N, Ruhoff AJ (2015) Characterizing the protonation states of the catalytic residues in apo and substrate-bound human T-cell leukemia virus type 1 protease. Comput Biol Chem 56:61–70. https://doi.org/10.1016/j.compbiolchem.2015.04.002
118. Kocak A, Erol I, Yildiz M, Can H (2016) Computational insights into the protonation states of catalytic dyad in BACE1-acyl guanidine based inhibitor complex. J Mol Graph Model 70:226–235. https://doi.org/10.1016/j.jmgm.2016.10.013
119. Chakravorty DK, Wang B, Ucisik MN, Merz KM Jr (2011) Insight into the cation-π interaction at the metal binding site of the copper metallochaperone CusF. J Am Chem Soc 133 (48):19330–19333. https://doi.org/10.1021/ja208662z
120. Zhou J, Xie H, Liu Z, Luo HB, Wu R (2014) Structure-function analysis of the conserved tyrosine and diverse π-stacking among class I histone deacetylases: a QM (DFT)/MM MD study. J Chem Inf Model 54(11):3162–3171. https://doi.org/10.1021/ci500513n
121. Lenz SAP, Wetmore SD (2017) QM/MM study of the reaction catalyzed by alkyladenine DNA glycosylase: examination of the substrate specificity of a DNA repair enzyme. J Phys Chem B 121(49):11096–11108. https://doi.org/10.1021/acs.jpcb.7b09646
122. Zhou J, Wang YS (2017) Rational redesign of a cation···π···π stacking at cardiovascular Fbw7-Skp1 complex interface and its application for deriving self-inhibitory peptides to disrupt the complex interaction. J Mol Model 23(10):296. https://doi.org/10.1007/s00894-017-3456-z
123. Zhang L, Hao GF, Tan Y, Xi Z, Huang MZ, Yang GF (2009) Bioactive conformation analysis of cyclic imides as protoporphyrinogen oxidase inhibitor by combining DFT calculations, QSAR and molecular dynamic simulations. Bioorg Med Chem 17

(14):4935–4942. https://doi.org/10.1016/j.bmc.2009.06.003

124. Mandal M, Zhu Z, Cumming JN, Liu X, Strickland C, Mazzola RD, Caldwell JP, Leach P, Grzelak M, Hyde L, Zhang Q, Terracina G, Zhang L, Chen X, Kuvelkar R, Kennedy ME, Favreau L, Cox K, Orth P, Buevich A, Voigt J, Wang H, Kazakevich I, McKittrick BA, Greenlee W, Parker EM, Stamford AW (2012) Design and validation of bicyclic iminopyrimidinones as beta amyloid cleaving enzyme-1 (BACE1) inhibitors: conformational constraint to favor a bioactive conformation. J Med Chem 55 (21):9331–9345. https://doi.org/10.1021/jm301039c
125. Arooj M, Sakkiah S, Kim S, Arulalapperumal V, Lee KW (2013) A combination of receptor-based pharmacophore modeling & QM techniques for identification of human chymase inhibitors. PLoS One 8 (4):e63030. https://doi.org/10.1371/journal.pone.0063030
126. Pasha FA, Neaz MM (2013) Molecular dynamics and QM/MM-based 3D interaction analyses of cyclin-E inhibitors. J Mol Model 19(2):879–891. https://doi.org/10.1007/s00894-012-1620-z
127. Bembenek SD, Keith JM, Letavic MA, Apodaca R, Barbier AJ, Dvorak L, Aluisio L, Miller KL, Lovenberg TW, Carruthers NI (2008) Lead identification of acetylcholinesterase inhibitors-histamine H3 receptor antagonists from molecular modeling. Bioorg Med Chem 16(6):2968–2973. https://doi.org/10.1016/j.bmc.2007.12.048
128. Remko M, Remková A, Broer R (2016) Theoretical study of molecular structure and physicochemical properties of novel factor Xa inhibitors and dual factor Xa and factor IIa inhibitors. Molecules 21(2):185. https://doi.org/10.3390/molecules21020185
129. Pardhi T, Vasu K (2018) Identification of dual kinase inhibitors of CK2 and GSK3β: combined qualitative and quantitative pharmacophore modeling approach. J Biomol Struct Dyn 36(1):177–194. https://doi.org/10.1080/07391102.2016.1270856
130. Spiegel K, Magistrato A (2006) Modeling anticancer drug-DNA interactions via mixed QM/MM molecular dynamics simulations. Org Biomol Chem 4(13):2507–2517. https://doi.org/10.1039/b604263p
131. Lodola A, Capoferri L, Rivara S, Chudyk E, Sirirak J, Dyguda-Kazimierowicz E, Andrzej Sokalski W, Mileni M, Tarzia G, Piomelli D, Mor M, Mulholland AJ (2011) Understanding the role of carbamate reactivity in fatty acid amide hydrolase inhibition by QM/MM mechanistic modelling. Chem Commun (Camb) 47(9):2517–2519. https://doi.org/10.1039/c0cc04937a
132. Schmidt TC, Welker A, Rieger M, Sahu PK, Sotriffer CA, Schirmeister T, Engels B (2014) Protocol for rational design of covalently interacting inhibitors. ChemPhysChem 15 (15):3226–3235. https://doi.org/10.1002/cphc.201402542
133. Capoferri L, Lodola A, Rivara S, Mor M (2015) Quantum mechanics/molecular mechanics modeling of covalent addition between EGFR-cysteine 797 and N-(4-anilinoquinazolin-6-yl) acrylamide. J Chem Inf Model 55(3):589–599. https://doi.org/10.1021/ci500720e
134. Ren W, Pengelly R, Farren-Dai M, Shamsi Kazem Abadi S, Oehler V, Akintola O, Draper J, Meanwell M, Chakladar S, Świderek K, Moliner V, Britton R, Gloster TM, Bennet AJ (2018) Revealing the mechanism for covalent inhibition of glycoside hydrolases by carbasugars at an atomic level. Nat Commun 9(1):3243. https://doi.org/10.1038/s41467-018-05702-7
135. James C, Pettit GR, Nielsen OF, Jayakumar VS, Joe IH (2008) Vibrational spectra and ab initio molecular orbital calculations of the novel anti-cancer drug combretastatin A-4 prodrug. Spectrochim Acta A Mol Biomol Spectrosc 70(5):1208–1216. https://doi.org/10.1016/j.saa.2007.10.052
136. Karaman R (2011) Computational-aided design for dopamine prodrugs based on novel chemical approach. Chem Biol Drug Des 78(5):853–863. https://doi.org/10.1111/j.1747-0285.2011.01208.x
137. Karaman R, Fattash B, Qtait A (2013) The future of prodrugs - design by quantum mechanics methods. Expert Opin Drug Deliv 10(5):713–729. https://doi.org/10.1517/17425247.2013.786699
138. Arfeen M, Patel DS, Abbat S, Taxak N, Bharatam PV (2014) Importance of cytochromes in cyclization reactions: quantum chemical study on a model reaction of proguanil to cycloguanil. J Comput Chem 35 (28):2047–2055. https://doi.org/10.1002/jcc.23719
139. Ponte F, Russo N, Sicilia E (2018) Insights from computations on the mechanism of reduction by ascorbic acid of Pt^{IV} prodrugs with asplatin and its chlorido and bromido analogues as model systems. Chemistry 24 (38):9572–9580. https://doi.org/10.1002/chem.201800488
140. Van der Kamp MW, Chaudret R, Mulholland AJ (2013) QM/MM modelling of ketosteroid isomerase reactivity indicates that active

site closure is integral to catalysis. FEBS J 280 (13):3120–3131. https://doi.org/10.1111/febs.12158

141. Kaiyawet N, Lonsdale R, Rungrotmongkol T, Mulholland AJ, Hannongbua S (2015) High-level QM/MM calculations support the concerted mechanism for Michael addition and covalent complex formation in thymidylate synthase. J Chem Theory Comput 11 (2):713–722. https://doi.org/10.1021/ct5005033
142. Kumari M, Kozmon S, Kulhánek P, Štepán J, Tvaroška I, Koča J (2015) Exploring reaction pathways for O-GlcNAc transferase catalysis. A string method study. J Phys Chem B 119 (12):4371–4381. https://doi.org/10.1021/jp511235f
143. Fernandes HS, Ramos MJ, Cerqueira NMFSA (2017) The catalytic mechanism of the pyridoxal-5′-phosphate-dependent enzyme, histidine decarboxylase: a computational study. Chemistry 23(38):9162–9173. https://doi.org/10.1002/chem.201701375
144. Elsässer B, Zauner FB, Messner J, Soh WT, Dall E, Brandstetter H (2017) Distinct roles of catalytic cysteine and histidine in the protease and ligase mechanisms of human legumain as revealed by DFT-based QM/MM simulations. ACS Catal 7(9):5585–5593. https://doi.org/10.1021/acscatal.7b01505
145. Roy S, Kästner J (2017) Catalytic mechanism of salicylate dioxygenase: QM/MM simulations reveal the origin of unexpected regioselectivity of the ring cleavage. Chemistry 23 (37):8949–8962. https://doi.org/10.1002/chem.201701286
146. Brás NF, Fernandes PA, Ramos MJ (2018) Understanding the rate-limiting step of glycogenolysis by using QM/MM calculations on human glycogen phosphorylase. ChemMedChem 13(15):1608–1616. https://doi.org/10.1002/cmdc.201800218
147. Lonsdale R, Houghton KT, Żurek J, Bathelt CM, Foloppe N, de Groot MJ, Harvey JN, Mulholland AJ (2013) Quantum mechanics/molecular mechanics modeling of regioselectivity of drug metabolism in cytochrome P450 2C9. J Am Chem Soc 135 (21):8001–8015. https://doi.org/10.1021/ja402016p
148. Tyzack JD, Williamson MJ, Torella R, Glen RC (2013) Prediction of cytochrome P450 xenobiotic metabolism: tethered docking and reactivity derived from ligand molecular orbital analysis. J Chem Inf Model 53 (6):1294–1305. https://doi.org/10.1021/ci400058s
149. Lonsdale R, Rouse SL, Sansom MS, Mulholland AJ (2014) A multiscale approach to modelling drug metabolism by membrane-bound cytochrome P450 enzymes. PLoS Comput Biol 10(7):e1003714. https://doi.org/10.1371/journal.pcbi.1003714
150. Putkaradze N, Kiss FM, Schmitz D, Zapp J, Hutter MC, Bernhardt R (2017) Biotransformation of prednisone and dexamethasone by cytochrome P450 based systems - identification of new potential drug candidates. J Biotechnol 242:101–110. https://doi.org/10.1016/j.jbiotec.2016.12.011
151. Ferreira AM, Krishnamurthy M, Moore BM II, Finkelstein D, Bashford D (2009) Quantitative structure-activity relationship (QSAR) for a series of novel cannabinoid derivatives using descriptors derived from semi-empirical quantum-chemical calculations. Bioorg Med Chem 7(6):2598–2606. https://doi.org/10.1016/j.bmc.2008.11.059
152. Güssregen S, Matter H, Hessler G, Müller M, Schmidt F, Clark T (2012) 3D-QSAR based on quantum-chemical molecular fields: toward an improved description of halogen interactions. J Chem Inf Model 52 (9):2441–2453. https://doi.org/10.1021/ci300253z
153. Ginex T, Muñoz-Muriedas J, Herrero E, Gibert E, Cozzini P, Luque FJ (2016) Application of the quantum mechanical IEF/PCM-MST hydrophobic descriptors to selectivity in ligand binding. J Mol Model 22 (6):136. https://doi.org/10.1007/s00894-016-2991-3
154. Hudson BD, Whitley DC, Ford MG, Swain M, Essex JW (2008) Pattern recognition based on color-coded quantum mechanical surfaces for molecular alignment. J Mol Model 14(1):49–57. https://doi.org/10.1007/s00894-007-0251-2
155. Vázquez J, Deplano A, Herrero A, Ginex T, Gibert E, Rabal O, Oyarzabal J, Herrero E, Luque FJ (2018) Development and validation of molecular overlays derived from three-dimensional hydrophobic similarity with PharmScreen. J Chem Inf Model 58 (8):1596–1609. https://doi.org/10.1021/acs.jcim.8b00216
156. Cannizzaro CE, Ashley JA, Janda KD, Houk KN (2003) Experimental determination of the absolute enantioselectivity of an antibody-catalyzed Diels-Alder reaction and theoretical explorations of the origins of stereoselectivity. J Am Chem Soc 125 (9):2489–2506. https://doi.org/10.1021/ja020879d

157. Smith AJT, Müller R, Toscano MD, Kast P, Hellinga HW, Hilvert D, Houk KN (2008) Structural reorganization and preorganization in enzyme active sites: comparisons of experimental and theoretically ideal active site geometries in the multistep serine esterase reaction cycle. J Am Chem Soc 130 (46):15361–15373. https://doi.org/10.1021/ja803213p

158. Frushicheva MP, Cao J, Chu ZT, Warshel A (2010) Exploring challenges in rational enzyme design by simulating the catalysis in artificial kemp eliminase. Proc Natl Acad Sci U S A 107(39):16869–16874. https://doi.org/10.1073/pnas.1010381107

159. Singh MK, Chu ZT, Warshel A (2014) Simulating the catalytic effect of a designed mononuclear zinc metalloenzyme that catalyzes the hydrolysis of phosphate triesters. J Phys Chem B 118(42):12146–12152. https://doi.org/10.1021/jp507592g